Journal of Power Sources 194 (2009) 674–682

Contents lists available at ScienceDirect

Journal of Power Sources

journal homepage: www.elsevier.com/locate/jpowsour

Direct methanol fuel cell performance of sulfonated polyimide membranes

Zhaoxia Hu[a,1], Takahiro Ogou[a,1], Makoto Yoshino[b], Otoo Yamada[a,1], Hidetoshi Kita[a,1], Ken-Ichi Okamoto[a,*]

[a] Graduate School of Science & Engineering, Yamaguchi University, Tokiwadai 2-16-1, Ube, Yamaguchi 755-8611, Japan
[b] Device & Materials Laboratories, Fujitsu Laboratories Ltd., 10-1, Morinosato-Wakamiya, Atsugi, Kanagawa, 243-0197, Japan

ARTICLE INFO

Article history:
Received 19 March 2009
Received in revised form 13 May 2009
Accepted 12 June 2009
Available online 4 July 2009

Keywords:
Direct methanol fuel cells
Sulfonated polyimides
Methanol crossover
Water crossover

ABSTRACT

Sulfonated polyimides (SPIs) derived from 1,4,5,8-naphthalene tetracarboxylic dianhydride, 4,4′-bis(4-aminophenoxy) biphenyl-3,3′-disulfonic acid and hydrophobic aromatic diamines showed the much lower methanol permeability and the lower proton conductivity than Nafion 112. The performance and the water and methanol crossover for direct methanol fuel cells (DMFCs) with the SPI membranes were investigated in comparison with Nafion membranes. The methanol and water fluxes increased significantly with increasing load current density for Nafion membranes but not for the SPI membranes, indicating that they were controlled by both the electro-osmotic drag and the molecular diffusion for the former but by only the molecular diffusion for the latter. These resulted in the much better DMFC performance for the SPIs than Nafion membranes especially at high methanol feed concentrations. The Faraday's efficiency and overall DMFC efficiency at 60 °C and 200 mA cm^{-2} for SPI membrane with IEC of 1.51 meq g^{-1} were 75% and 21%, respectively, at 5 wt.% methanol feed concentration, and 36% and 9.5%, respectively, at 20 wt.% methanol concentration. They were about two times and three times higher at 5 wt.% and 20 wt.% methanol concentrations, respectively, than those for Nafion 112. The short-term durability test for 300 h at 60 °C revealed no deterioration in the DMFC performance. The SPI membranes have high potential for DMFC applications at mediate temperatures (40–80 °C).

1. Introduction

Direct methanol fuel cells (DMFCs) have been drawing great attention because of their potential use as future energy sources for ubiquitous portable devices such as laptop and mobile phone [1,2]. Aqueous methanol solution is used as the fuel to generate electrical power in a DMFC instead of hydrogen gas, which has the advantage of making the whole system both compact and simple. It is crucial to use concentrated fuel to achieve high level of energy capacity, which gives rise to the large methanol crossover through a polymer electrolyte membrane (PEM) from anode to cathode. The methanol crossover in DMFC results not only in fuel loss, but also in an increase in air demand and in a decrease of cell efficiency, due to the reactions and depolarization of permeated methanol with oxygen at the cathode [3–7]. Because of the issue of methanol crossover as well as the high cost, the state-of-the-art perfluorosulfonic acid membranes such as DuPont's Nafion are not suitable for DMFC applications. In the past decades, there have been reported a lot of literatures focusing on alternative aromatic PEM materials [8–22] such as sulfonated poly(aryl ether)s (SPAEs) [9–13], sulfonated poly(ether ether ketone)s (SPEEKs) [14,15], sulfonated polyimides (SPIs) [16–22], and so on. Besides the methanol crossover, the control of water level in a PEM also cannot be neglected, which would give considerable effects on the proton conductivity, fuel transport and electrode reaction kinetics [7,23]. The perfluorosulfonic acid membranes also showed the transport of a large amount of water through PEM in DMFC operation. Therefore, for the alternative PEMs, it is necessary to keep an optimum maintenance of water balance to achieve high fuel cell performance.

Most of the alternative PEMs mentioned above have been reported to have comparable or slightly lower proton conductivity in water but much lower methanol permeability compared with Nafion, resulting in much larger selectivity of proton conductivity to methanol crossover. However, most of the researches have dealt with methanol permeability measured by a liquid/liquid permeation method ($p_{M,L/L}$). Only several researches have dealt with the *in situ* analysis of the methanol crossover in DMFC operation [5,6,9,13,17,20,21]. Furthermore, only a few researches have dealt with the *in situ* analysis of both the methanol and water crossover during DMFC operation [9,20].

SPI membranes are considered as one of the promising candidates due to their good film-forming ability and low fuel

* Corresponding author. Tel.: +81 836 85 9660; fax: +81 836 85 9601.
E-mail addresses: okamotok@yamaguchi-u.ac.jp, okamotok@po.cc.yamaguchi-u.acv.jp (K.-I. Okamoto).
[1] Tel.: +81 836 85 9660; fax: +81 836 85 9601.

0378-7753/$ – see front matter © 2009 Elsevier B.V. All rights reserved.
doi:10.1016/j.jpowsour.2009.06.086

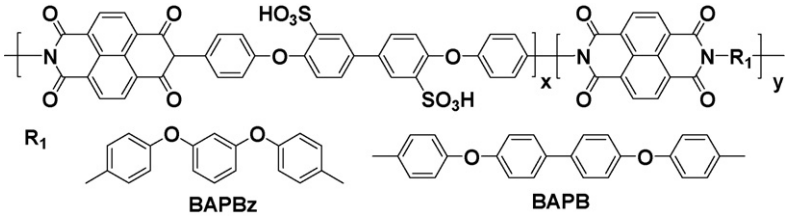

Fig. 1. Chemical structure of SPIs from NTDA and BAPBDS.

crossover [16–22,24,25]. If the ion exchange capacity (IEC) is beyond a certain level, for example 1.5 mequiv. g^{-1}, some PEMs such as SPAE and SPEEK swelled extremely or dissolved into methanol. On the contrary, the SPI membranes showed much stronger tolerance towards methanol, namely they slightly swelled when soaked in methanol. We have reported some preliminary works about methanol permeability $p_{M,L/L}$ for SPIs derived from 1,4,5,8-naphthalene tetracarboxylic dianhydride (NTDA), sulfonated and non-sulfonated diamines with relatively high IECs of 1.8–2.3 mequiv. g^{-1} [19]. Our results showed that the $p_{M,L/L}$ of the SPI membranes hardly depended on the methanol concentration up to 50 wt.%. The $p_{M,L/L}$ values were in the range of 0.5×10^{-6} cm^2 s^{-1} to 1.7×10^{-6} cm^2 s^{-1} at 50 °C and more than two times smaller than those of Nafion 112. In addition to the high methanol tolerance, the excellent membrane stability is also required for PEMs. The SPIs based on sulfonated diamine of 4,4′-bis(4-aminophenoxy) biphenyl-3,3′-disulfonic acid (BAPBDS) showed the high water stability, that is, they maintained the high proton conductivity and tensile strength after aging in water at 130 °C for 300 h, suggesting high potential as PEMs with the durability of more than 20,000 h at temperatures below 80 °C [26].

In this paper, we prepare a series of SPI membranes from NTDA and BAPBDS with IECs of 1.51–1.96 mequiv. g^{-1}, of which the chemical structure is shown in Fig. 1, and investigate their fuel cell performances in comparison with Nafion, including methanol and water crossover during DMFC operation.

2. Experimental

2.1. Membrane preparation and characterization

The random copolyimides were prepared from NTDA, BAPBDS and 1,3-bis(4-aminophenoxy) benzene (BAPBz) or 4,4′-bis(4-aminophenoxy) biphenyl (BAPB) by one-pot high temperature polycondensation according to the reported method [16,24,25]. Tough and flexible SPI membranes were obtained by casting their 5–6 wt.% *m*-cresol solutions (in triethylamine form) onto glass plates, followed by residue extraction in methanol and proton exchange in 1 M hydrochloric acid solution [24,25].

The IEC of SPIs was calculated from the feed molar ratio of the sulfonated diamine to the non-sulfonated one. Water uptake and dimensional change of membrane were measured according to the methods described elsewhere [24]. Water uptake was measured by immersing a sample sheet into water at 30 °C for 5 h. Then, the membrane was taken out, wiped with tissue paper very quickly, and weighed on a microbalance. Water uptake (*WU*) was calculated from Eq. (1):

$$WU\,(\%) = \frac{W_s - W_d}{W_d} \times 100 \tag{1}$$

where W_d and W_s are the weights of dry and corresponding water-swollen membranes, respectively.

Dimensional changes in thickness (Δt_c) and in plane direction (Δl_c) were investigated by immersing more than two sample sheets in water at 30 °C for 5 h. The changes of thickness and length were calculated from Eq. (2):

$$\Delta t_c = \frac{t - t_d}{t_d}$$
$$\Delta l_c = \frac{l - l_d}{l_d} \tag{2}$$

where t_d and l_d are the thickness and length of the dry membrane, respectively; t and l refer to those of the membrane swollen in water.

In-plane and *through-plane* proton conductivity ($\sigma_{//}$ and $\sigma_{\perp}$, respectively) of SPI membrane was determined using an electrochemical impedance spectroscopy technique over the frequency from 10 Hz to 100 kHz (Hioki 3532-80). For $\sigma_{//}$, a single cell with two platinum plate electrodes was mounted on a Teflon plate at 0.5 cm distance. For $\sigma_{\perp}$, a membrane sample was set between two platinum plate electrodes of 1 cm^2 area, and mounted on two Teflon blocks. The cell was placed in liquid water. Proton conductivity, $\sigma_{//}$ and $\sigma_{\perp}$, were calculated from Eq. (3):

$$\sigma_{//} = \frac{d}{twR}$$
$$\sigma_{\perp} = \frac{t}{AR} \tag{3}$$

where d is the distance between the two electrodes, t and w are the thickness and width of the water-swollen membrane, respectively, A is the electrode area, and R is the resistance value measured. In the *through-plane* conductivity measurement, the contact resistance between electrodes and membrane could be neglected only in the fully hydrated state. The similar $\sigma_{\perp}$ values were obtained for the samples of single layer and double layers of membrane.

Methanol permeability $p_{M,L/L}$ was measured by a liquid–liquid permeation method as described elsewhere [19]. The measurements were carried out by using a liquid permeation cell and measuring the methanol concentration in the feed and permeate at 60 °C with an initial methanol concentration in feed of 10 wt.%.

2.2. Fabrication of membrane electrode assembly (MEA) and measurements of cell performance

A MEA was fabricated using SPI or Nafion membrane as PEM. Pt70Ru30/C (54%, TEC61E54, Tanaka Kikinzoku Gr.) and Pt/C (45.5%, TEC10E50E, Tanaka Kikinzoku Gr.) were used as anode and cathode catalysts, respectively. The catalyst was dispersed uniformly into the mixture of appropriate amount of water, 1-propanol, 2-propanol, and Nafion® dispersion solution (21 wt.%, Aldrich) through ball-milling and degassing. The catalyst ink prepared thus was coated onto a carbon paper (Toray Indus. Inc., TGP-H-090, 0.28 mm) using a bar-coater, and dried to obtain a catalyst-coated electrode. The catalyst loadings for the anode and cathode were 2.2 mg Pt/Ru cm^{-2} and 1.67 mg Pt cm^{-2}, respectively. Both sides of the PEM surface were impregnated uniformly with 1.0 mg cm^{-2} of Nafion by applying 0.02 mL cm^{-2} of 5 wt.% Nafion solution as a

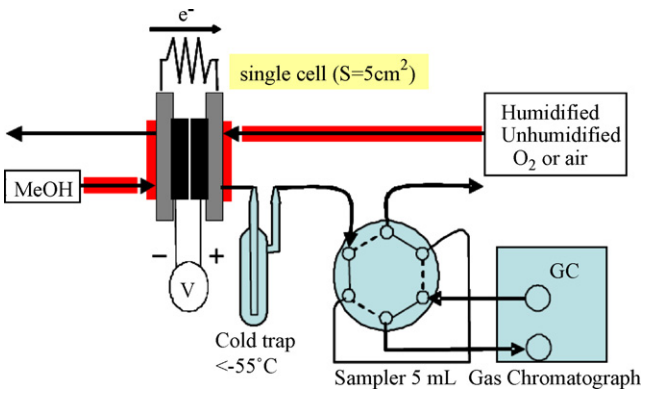

Fig. 2. Schematic diagram of measurement apparatus for water and methanol crossover in DMFC operation.

binder. A PEM was sandwiched between two catalyst electrodes and hot-pressed at 150 °C at 30 kgf cm^{-2} for 3 min. The effective electrode area was 5 cm^2. The prepared MEA was positioned into a single cell test fixture (JARI).

DMFC measurements were carried out in a DMFC test station (KIKUSUI KFM2030, EIWA) at 40–80 °C. An aqueous methanol solution (5–50 wt.%) was supplied into the anode at a flow rate of 1.0 mL min^{-1}, O_2 or air was supplied into the cathode at 150 N cm^3 min^{-1} or 150–750 N cm^3 min^{-1}, respectively, under air atmosphere. The gas was passed through a humidifier at a given temperature if necessary.

Alternating current (AC) impedance analysis was performed under steady-state conditions. The frequency range was from 0.1 Hz to 10 kHz and the load current was set at 0.25 A, 0.5 A, 1.0 A and 1.5 A. The cell resistance (R_c) and electrode reaction resistance (R_{el}) were determined by the AC impedance cole–cole plots. The proton conductivity in thickness direction of membrane ($\sigma_{\perp,FC}$) was evaluated by assuming that the membrane resistance is approximately equal to the cell resistance.

2.3. Measurements of methanol and water crossover during DMFC operation

The water and methanol crossover through PEM during fuel cell operation was measured using the apparatus depicted in Fig. 2. Most of the methanol permeated through a membrane was oxidized into CO_2 and water at the cathode. A small part of the methanol was not oxidized and flowed into the cathode outlet stream. The cathode effluent was conducted to a cold trap (<−60 °C) to condense the water and methanol vapor and then the dried gas was conducted to a gas sampler for the gas chromatography to measure the CO_2 content. The condensed liquid was weighed and then subjected to the gas chromatography to determine the methanol content. The methanol permeation flux (q_M) was calculated from Eq. (4):

$$q_M\,(\text{mol cm}^{-2}\,\text{s}^{-1}) = \frac{M_{CO_2} + M_{MeOH}}{At_{mea}} \quad (4)$$

where M_{CO_2} (mol) and M_{MeOH} (mol) are the CO_2 amount and the methanol amount, respectively, flowed into the cathode outlet stream for the measurement time, t_{mea}, and A is the effective area of MEA. The methanol permeation coefficient p_M was evaluated from Eq. (5), assuming that the membrane was in contact with the feed methanol solution and feed cathode gas:

$$p_M\,(\text{cm}^2\,\text{s}^{-1}) = \frac{q_M t_{50\%RH}}{C_M} \quad (5)$$

where C_M is a methanol concentration in feed and $t_{50\%RH}$ is the thickness of membrane under 50%RH. The water permeation flux (q_W) was calculated from Eq. (6):

$$q_W\,(\text{mol cm}^{-2}\,\text{s}^{-1}) = \frac{M_{WT} - M_{WR} - 2M_{CO_2}}{At_{mea}} \quad (6)$$

where M_{WT} (mol) is the amount of water trapped and M_{WR} (mol) the amount of water generated by the electrochemical reaction of proton at cathode for t_{mea}.

3. Results and discussion

3.1. Characterization of SPI membranes

In this study, four types of SPI membranes with the higher IECs (M1 and M2) and the lower ones (M3 and M4) were investigated and compared with Nafion membranes. Their physical properties are summarized in Table 1. All the SPIs had high molecular weights judging from their large reduced viscosities and gave ductile membranes of 30–65 μm in thickness. The SPI membranes displayed the anisotropic membrane swelling and proton conductivity. The dimensional change was about three times larger in the thickness direction than in the plane one. The $\sigma_\perp$ was about 25% smaller than the $\sigma_{//}$. These are because the polymer chains tend to align in the plane direction to some degree, as reported in a previous paper [27]. On the other hand, Nafion membranes showed the isotropic membrane swelling and proton conductivity. At 60 °C, the SPIs showed slightly lower conductivity values in water than Nafion 112. According to liquid–liquid permeation measurements, Nafion 112 showed high $p_{M,L/L}$ values of 4.4×10^{-6} cm^2 s^{-1} and 2.4×10^{-6} cm^2 s^{-1} at 60 °C and 30 °C, respectively, for 10 wt.% methanol solution, which were comparable to those reported for Nafion membranes ($2.0–3.2 \times 10^{-6}$ cm^2 s^{-1} at 23–30 °C) [7,8]. On the other hand, the SPI membrane M2 showed a much lower $p_{M,L/L}$ value of 1.66×10^{-6} cm^2 s^{-1} at 60 °C for 10 wt.% methanol. As a result, the selectivity ($\sigma_\perp/p_{M,L/L}$) values were 5.4×10^4 S cm^{-3} s^{-1}

Table 1
IEC, water uptake (*WU*), methanol uptake (*MU*), size change (Δt_c, Δl_c) and proton conductivity ($\sigma_{//}$, $\sigma_\perp$) of SPI and Nafion 112 membranes.

Code	SPIs[a]	Thickness (μm)	IEC[b] (mequiv. g^{-1})	η_r[c] (dL g^{-1})	*WU*[d] (%)	*MU*[d] (%)	Size change[d]		$\sigma_{//}$[e] (mS cm^{-1})	$\sigma_\perp$[e]
							Δt_c	Δl_c		
M1	BAPBz(2/1)	46	1.96	4.4	60		0.21	0.084	127	–
M2	BAPB(2/1)	34	1.89	4.9	57	51	0.18	0.061	127	93
M3	BAPBz(1/1)	65	1.56	2.3	44	47	0.17	0.055	78	60
M4	BAPB(1/1)	53	1.51	4.4	46	44	0.16	0.057	86	64
Nafion 112		55	0.91	–	39	81	0.14	0.13	139	136

[a] Derived from NTDA, BAPBDS and non-sulfonated diamines, BAPB or BAPBz. The data in parentheses are the molar ratios of BAPBDS to non-sulfonated diamine.
[b] Theoretical value.
[c] 0.5 g/dL at 35 °C in *m*-cresol.
[d] At 30 °C.
[e] At 60 °C in water.

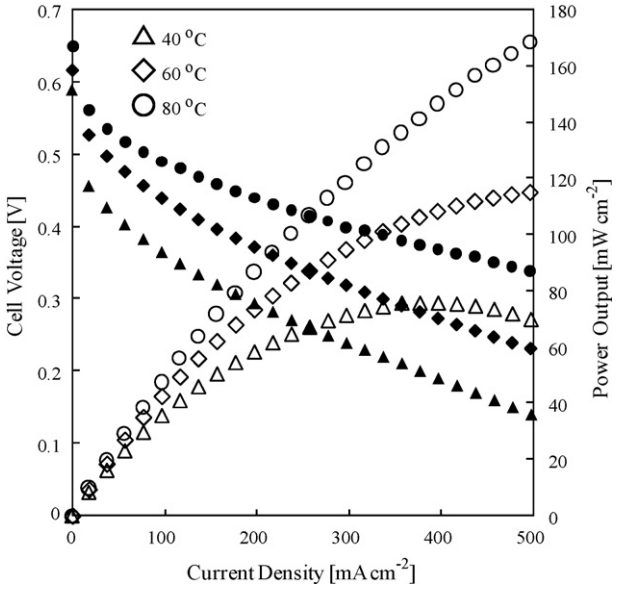

Fig. 3. Effects of cell temperature on DMFC performance for M2 with supply of 5 wt.% methanol solution and O_2 (150 N cm^3 min^{-1}, dry).

and 3.2×10^4 S cm^{-3} s^{-1} for M2 and Nafion 112, respectively. The former was 1.7 times larger than the latter.

3.2. DMFC performance

Fig. 3 shows the effects of cell temperature on DMFC performance for M2 with supplying 5 wt.% methanol solution and dry oxygen. With increasing cell temperature from 40 °C to 80 °C, the DMFC performance significantly increased. For example, the open circuit voltage (*OCV*) increased from 0.59 V at 40 °C to 0.65 V at 80 °C and the cell voltage at current density of 200 mA cm^{-2} (V_{200}) increased from 0.29 V to 0.44 V. This was due to that the positive effect of an enhancement in the electrode reaction rate with an increase in cell temperature was more predominant than the negative effect of an increase in the methanol crossover. In this study, the fuel cell properties at 60 °C were investigated in detail.

Fig. 4 shows the effects of cathode gas and its flow rate on DMFC performance for M2 at methanol feed concentrations of 5 wt.%, 10 wt.% and 30 wt.%. The preliminary experiments for 5 wt.% methanol were carried out by varying the humidification conditions of cathode gas. The gas humidified at 25 °C gave the similar results to those shown in Fig. 4(a) for the dry gas, whereas the gas humidified at 50 °C gave the lower performance. Therefore, in this study, the cathode gas was supplied without the humidification. In the case of oxygen supply, the DMFC performance hardly depended on the flow rate above 30 N cm^3 min^{-1}. In the case of air supply, the behavior was somewhat different depending on the methanol feed concentration. At 5 wt.% methanol feed concentration, in the low current density range up to 200 mA cm^{-2}, the cell voltage was almost the same in magnitude between the oxygen and air supply regardless of the flow rate, for example, 0.45 V at 100 mA cm^{-2} for every case. With increasing current density above 200 mA cm^{-2}, the cell voltage decreased more largely for air than for oxygen. As a result, the cell voltages at 400 mA cm^{-2} were 0.29 V for oxygen and 0.25 V for air at 750 N cm^3 min^{-1} and 450 N cm^3 min^{-1}. With air supply at 150 N cm^3 min^{-1}, the cell voltage largely dropped in the current density range above 300 mA cm^{-2}. This was because the oxygen gas diffusion process at the cathode became the rate-determining step. At 10 wt.% methanol feed concentration, the cell voltage was smaller for air than for oxygen even in the low current density range. For example, V_{200} was 0.37 V for oxygen and 0.33 V

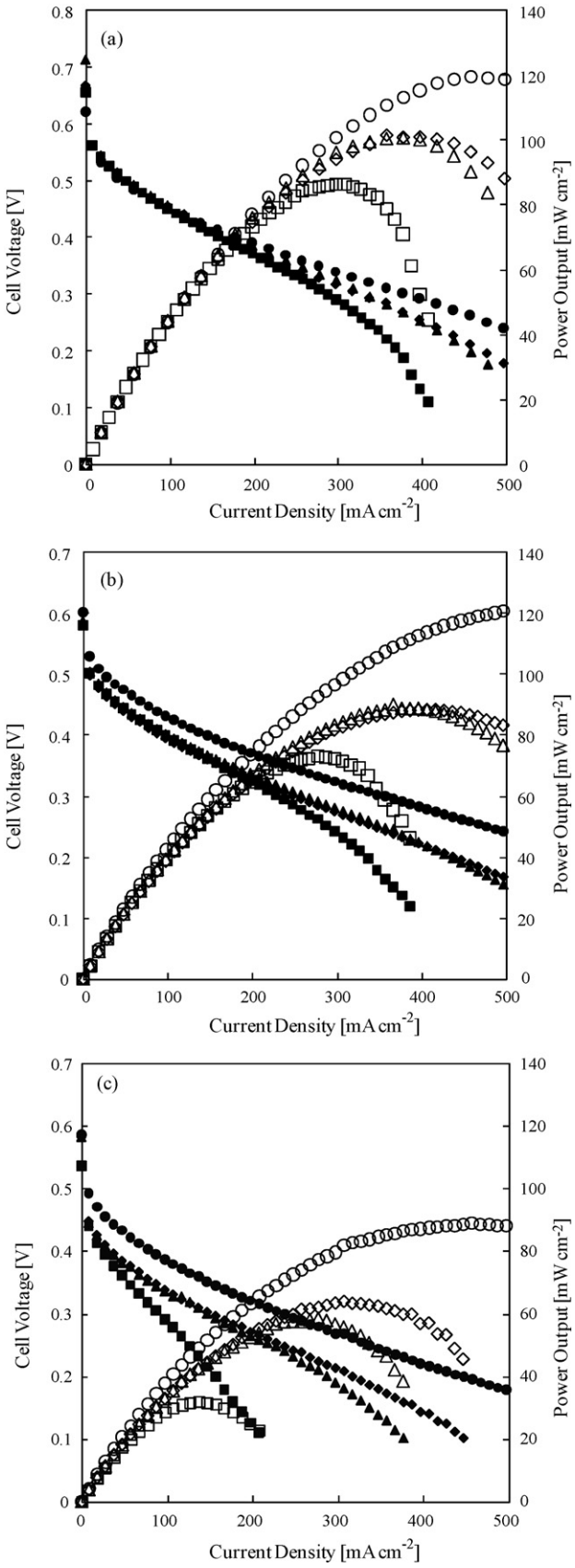

Fig. 4. Effects of cathode gas and its flow rate on DMFC performance for M2 at 60 °C with supply of (a) 5 wt.%, (b) 10 wt.%, and (c) 30 wt.% methanol solutions and dry gas. (○, ●) O_2, 150 N cm^3 min^{-1}; (◇, ♦) air, 750 N cm^3 min^{-1}; (△, ▲) air, 450 N cm^3 min^{-1}; (□, ■) air, 150 N cm^3 min^{-1}.

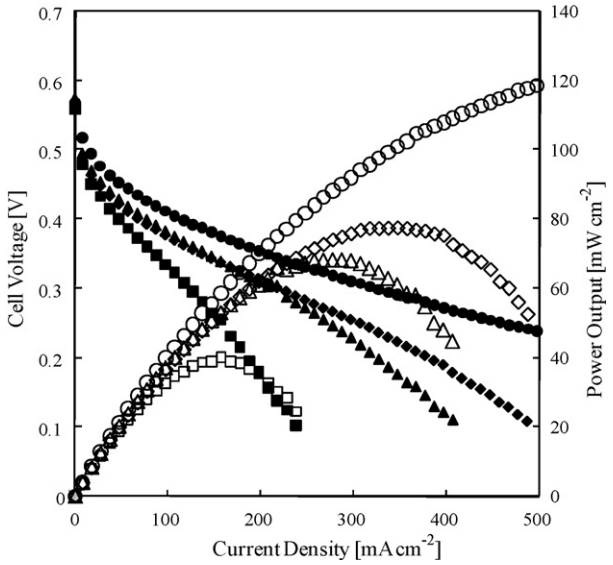

Fig. 5. Effects of cathode gas and its flow rate on DMFC performance for Nafion 112 at 60 °C with supply of 10 wt.% methanol solution and dry gas. (○, ●) O_2, 150 N cm^3 min^{-1}; (◊, ♦) air, 750 N cm^3 min^{-1}; (△, ▲) air, 450 N cm^3 min^{-1}; (□, ■) air, 150 N cm^3 min^{-1}.

for air at every flow rate. The difference in the cell voltage became larger with increasing current density. At 30 wt.% methanol feed concentration, the difference in the cell voltage between the oxygen and air supply was larger, especially for the low flow rate of 150 N cm^3 min^{-1}, than that at 10 wt.% methanol one. The cell voltages at 100 mA cm^{-2} were 0.39 V for oxygen and 0.34 V and 0.29 V for air at 750 N cm^3 min^{-1} (450) and 150 N cm^3 min^{-1}, respectively. The effects of air supply and its flow rate on the cell performance were much larger at the higher methanol concentration and the higher current density. The results mentioned above in Figs. 3 and 4 were also observed for the other SPI membranes.

Fig. 5 shows the effects of cathode gas and its flow rate on DMFC performance for Nafion 112. The large effects of the air supply and its flow rate were observed for Nafion 112 at 10 wt.% methanol feed concentration. The behavior was comparable to that for M2 at 30 wt.% methanol concentration. The cell performance for Nafion 112 could not be measured with supply of 30 wt.% methanol solution and air.

Effects of methanol feed concentration on the DMFC performance with oxygen supply at a flow rate of 150 N cm^3 min^{-1} for M4 and Nafion 112 are shown in Figs. 6(a) and 7(a), respectively. At a low methanol concentration of 5 wt.%, M4 and Nafion 112 showed the similar cell performance except for *OCV*; that is, the *OCV*, cell voltage at 200 mA cm^{-2} (V_{200}) and maximum output (W_{max}) were 0.69 V, 0.40 V and 120 mW cm^{-2}, respectively, for M4, whereas 0.61 V, 0.38 V and 126 mW cm^{-2} for Nafion 112. With an increase in methanol feed concentration up to 30 wt.%, the cell performance decreased less for M4 than for Nafion 112. As a result, at 30 wt.% methanol concentration, M4 kept a high W_{max} of 83 mW cm^{-2}, which was 2.3 times larger than that for Nafion 112. The DMFC with Nafion 112 did not work stably at 50 wt.% methanol feed concentration, whereas M4 still kept fairly high cell performance, namely, *OCV* of 0.61 V, V_{200} of 0.32 V and W_{max} of 70 mW cm^{-2}.

Figs. 6(b) and 7(b) show effects of methanol feed concentration on the cell performance with air supply at a flow rate of 450 N cm^3 min^{-1} for M4 and Nafion 112, respectively. Compared with the oxygen supply, the air supply reduced the cell performance largely. The reduction in cell performance was larger for Nafion 112 than for M4 and for higher methanol concentration. At 10 wt.% methanol concentration, the W_{max} values were 83 mW cm^{-2} and

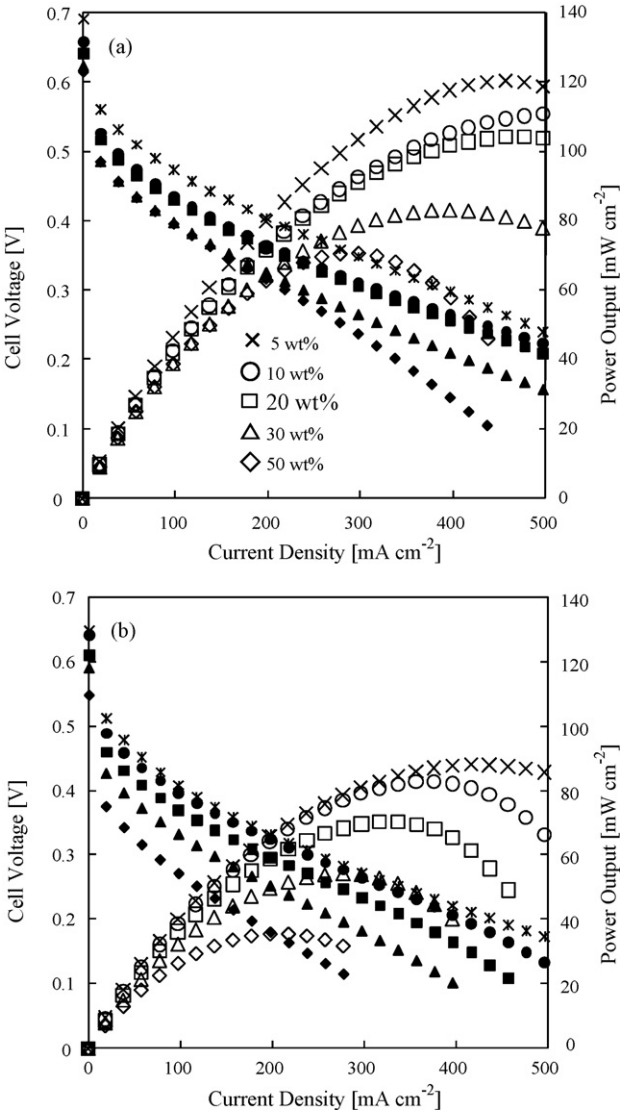

Fig. 6. Effects of methanol feed concentration on DMFC performance for M4 with supply of (a) O_2 (150 N cm^3 min^{-1}) and (b) air (450 N cm^3 min^{-1}) at 60 °C.

68 mW cm^{-2} for M4 and Nafion 112, respectively, which were 25% and 40% lower than those with the oxygen supply. At 30 wt.% methanol concentration, Nafion 112 showed the too low cell performance to be measured stably, whereas M4 displayed moderately high cell performance, namely, *OCV* of 0.59 V, V_{200} of 0.25 V and W_{max} of 55 mW cm^{-2}.

3.3. Methanol and water crossover

Fig. 8(a) and (b) shows the methanol and water crossover through M1, M4 and Nafion 115 during DMFC operation as functions of load current density and methanol feed concentration, respectively. Nafion 115 with a larger thickness of 130 μm was chosen here for comparison, considering the high methanol crossover for Nafion 112 at high methanol concentrations above 20 wt.%. In Fig. 8(a), with an increase in the current density at a constant methanol feed concentration of 20 wt.%, the water flux q_W for Nafion 115 increased significantly due to the increasing contribution of electro-osmotic drag of proton migration. From the slope of the line in the current range above 200 mA cm^{-2}, the water electro-osmotic drag coefficient for Nafion 115 was evaluated as 2.4 H_2O/H^+, which was close to the literature values of 2.5–3.3 H_2O/H^+ [20,28]. On the other

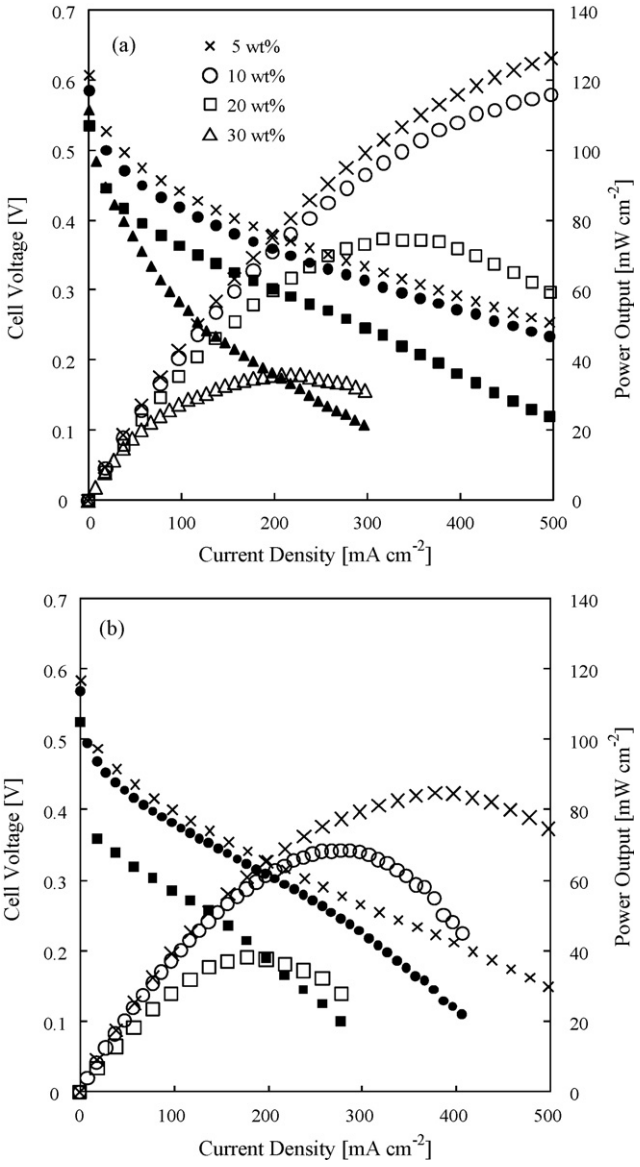

Fig. 7. Effects of methanol feed concentration on DMFC performance for Nafion 112 with supply of (a) O_2 (150 N cm^3 min^{-1}) and (b) air (450 N cm^3 min^{-1}) at 60 °C.

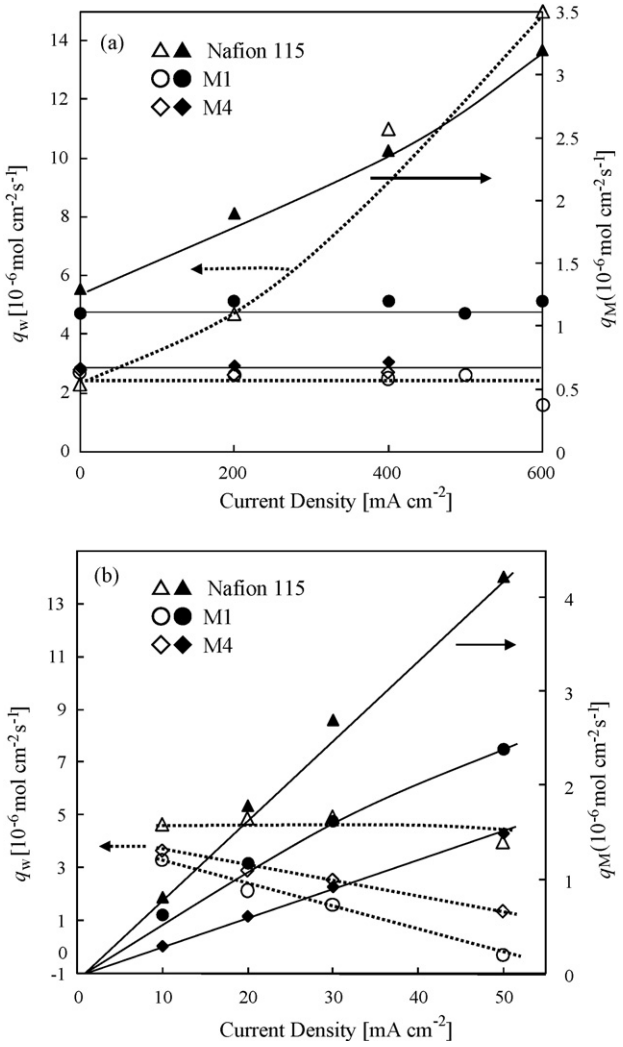

Fig. 8. Water flux (△, ○, ◊) and methanol flux (▲, ●, ♦) for DMFCs with Nafion 115, M1 and M4 at 60 °C with supply of O_2. (a) Effect of current density at 20 wt.% methanol feed concentration and (b) effect of methanol feed concentration at a current density of 200 mA cm^{-2}.

hand, the q_W for M1 and M4 hardly changed with an increase in the current density, indicating that the water flux was not controlled by the electro-osmotic drag but by the molecular diffusion. This seemed due to the difference in membrane morphology. The SPI membranes have no clear hydrophilic ionic channel structure as considered in Nafion membranes and have the lower fraction of loosely bonded and free water than Nafion membranes. The similar water crossover behavior has been reported for disulfonated poly(arylene ether benzonitrile)s [9]. In Fig. 8(b) at a constant current density of 200 mA cm^{-2}, the q_W for Nafion 115 hardly changed with an increase in the methanol concentration, because it was controlled by the electro-osmotic drag. On the other hand, for M1 and M4, the q_W decreased largely with an increase in the methanol concentration (or with a decrease in the water concentration at anode), because of a decrease in the driving force of water diffusion.

The ratio of unoxidized methanol in the cathode outlet stream to the total methanol permeated through the membrane was 3–9% for Nafion 112 and 0.5–2.5% for Nafion 115 and SPI membranes at methanol feed concentrations of 5–30 wt.% and at 200 mA cm^{-2}. In this paper, the CO_2 amount in the cathode outlet stream was attributed only to the methanol crossover, because the contribution of the CO_2-crossover from the anode was considered to be negligibly small in the case of high methanol concentrations above 5 wt.% and the low current densities, based on the reported results [29].

In Fig. 8(a), with increasing the current density from 0 mA cm^{-2} up to 600 mA cm^{-2}, the methanol flux q_M for Nafion 115 increased largely from 1.3×10^{-6} mol cm^{-2} s^{-1} up to 3.2×10^{-6} mol cm^{-2} s^{-1}. This indicated that the methanol crossover for Nafion membranes was controlled by both the molecular diffusion and the electro-osmotic drag. Recently, the relationship of leakage current density (or q_M) versus current density has been investigated for Nafion membranes as parameters of operational conditions such as cell temperature, methanol feed concentration, membrane thickness, and anode and cathode flow rates and the experimental results have been analyzed based on a model [5]. According to Eccarius et al., the q_M decreased with increasing the current density at a low methanol concentration of 1.6 wt.%, whereas it increased at 4.8 wt.% methanol concentration. According to their simulation results, for 12.8 wt.% methanol, the q_M increased largely with increasing the current density, as observed for 20 wt.% methanol in the present study. On the other hand, for the SPI membranes, the q_M hardly changed with the current density, indicating that the methanol crossover for SPI membranes was not controlled by the electro-osmotic drag but

Table 2
Methanol flux and permeability (q_M, p_M), proton conductivity ($\sigma_{\perp,FC}$), *OCV*, cell voltage ($V_{200(400)}$), potential efficiency (η_E), Faraday's efficiency (η_F) and overall DMFC efficiency (η_{DMFC}) of SPI and Nafion membranes during DMFC operation.

PEMs	MeOH (%)	q_M (μmol cm^{-2} s^{-1})	p_M ($\times 10^6$ cm^2 s^{-1})	$\sigma_{\perp FC}$ (mS cm^{-1})	*OCV* (mV)	$V_{200(400)}$ (mV)[b]	η_E (%)	η_F (%)	η_{DMFC} (%)
Nafion 112	5	0.53	1.87	62	588	361	30	40	11.2
Air[a]		0.53	1.9	62	585	329	27	40	10.8
M4		0.13(0.10)	0.44(0.33)	29	690	385(266)	32(22)	73(88)	23(19)
Air		0.12(0.10)	0.40(0.35)	28	670	340(221)	28(18)	75(87)	21(16)
Nafion 112	10	1.2	2.2	62	574	350	29	22	6.3
Nafion 115		0.88	3.7	84	610	372	31	28	8.6
Air		0.82	3.4	88	608	345	28	30	8.4
M2		0.64	0.71	39	640	413	34	35	12
M4		0.29(0.27)	0.5(0.47)	27	657	365(265)	30(22)	54(72)	16.3(15.6)
Air		0.29(0.33)	0.5(0.55)	26	643	325(207)	27(17)	54(68)	14.5(11.6)
Nafion 112	20	2.5	2.2	63	544	322	27	12	3.3
Nafion 115		2.0(2.5)	4.1(5.3)	78	562	330(237)	27(20)	15(21)	4.1(4.2)
M1		1.2	0.88	28	597	362	30	23	6.7
M3		0.55	0.57	19	580	307	25	38	9.2
M4		0.61(0.63)	0.52(0.53)	24	641	362(265)	30(22)	36(52)	10.8(11.4)
Air		0.63(0.76)	0.53(0.65)	23	611	325(164)	27(13.5)	36(48)	9.5(6.4)
Nafion 112	30	3.2	1.9	54	525	152	12.5	10	1.2
Nafion 115		3.0	4.1	74	581	301	25	10	2.6
M1		1.56	0.77	25	555	307	25	18	4.6
M4		0.92	0.52	21	613	318	26	27	7.1
Air		0.95	0.54	19	590	231	19	27	5.1
Nafion 115	50	4.6	3.9	68	533	136	11	7	0.8
M1		2.42	0.72	21	542	284	13	13	2.9
M4		1.53	0.52	18	613	322	26.5	18	4.9
Air		1.49	0.51	16	548	139	11.4	19	2.2

[a] With air supply at 450 N cm^3 min^{-1}.
[b] At 60 °C and 200 mA cm^{-2}; the data in parentheses are at 400 mA cm^{-2}; with oxygen supply at 150 N cm^3 min^{-1} unless noted as air.

by the molecular diffusion. As a result, the difference in methanol flux between Nafion and SPI membranes became much larger with increasing the current density. In Fig. 8(b), at a constant current density of 200 mA cm^{-2}, the q_M increased linearly with increasing the methanol concentration for Nafion and SPI membranes, indicating that the p_M hardly depended on the methanol concentration.

The q_M and p_M values measured *in situ* during DMFC operation are listed in Table 2. It is noted in this paper that the q_M and p_M refer to the values measured *in situ* during DMFC operation, whereas the $q_{M,L/L}$ and $p_{M,L/L}$ refer to the corresponding values measured *ex situ* by the liquid/liquid permeation method. It has been reported for Nafion membranes that the $q_{M,L/L}$ varies inversely as membrane thickness and the $p_{M,L/L}$ hardly depends on the thickness [7]. On the other hand, the q_M has been reported not to vary so largely as due to the contribution of the electro-osmotic drag [4], suggesting the larger p_M for the thicker Nafion membrane. In this study, the p_M value of Nafion 115 (4.0×10^{-6} cm^2 s^{-1}) was two times larger than that of Nafion 112 (2.0×10^{-6} cm^2 s^{-1}). On the other hand, for SPI membranes the q_M varied inversely as the thickness and the p_M hardly depended on the thickness. For example, M3 membranes with different thicknesses of 35 μm and 65 μm showed p_M values of 0.61×10^{-6} cm^2 s^{-1} and 0.57×10^{-6} cm^2 s^{-1}, respectively. This is because the molecular diffusion was dominant for the SPI membranes. Among the SPI membranes M1–M4, the methanol permeability depended mainly on the IEC. M1 with a high IEC of 1.96 mequiv. g^{-1} showed a high p_M value of about 0.9×10^{-6} cm^2 s^{-1}, whereas M4 with a low IEC of 1.51 mequiv. g^{-1} showed a low p_M value of about 0.5×10^{-6} cm^2 s^{-1}, which was a fourth of that of Nafion 112.

The q_M values and their measurement conditions reported in literatures are listed in Table 3 for comparison with our results. For Nafion membranes, the q_M values in this study were in the similar level to those reported by Eccarius et al. and Kim et al. [5,13], but were fairly larger than those reported by Kim et al. and Watanabe and co-workers [9,21]. From the data reported by Watanabe and co-workers and Kim et al. for Nafion 112, the q_M values at 60 °C and 5 wt.% methanol were evaluated as 0.13×10^{-6} mol cm^{-2} s^{-1} and 0.33×10^{-6} mol cm^{-2} s^{-1}, respectively, which were a quarter and two thirds, respectively, of our value, 0.53×10^{-6} mol cm^{-2} s^{-1}. The methanol crossover is also affected by the anode backing and catalyst layers. If these layers effectively disturb the methanol diffusion, the methanol concentration at the interface between the anode catalyst layer and the membrane will become lower than the feed concentration, and as a result the methanol crossover will be effectively reduced. The difference in the q_M values among the literatures and the present study might be attributed to some difference in the anode backing and catalyst layers. The q_M values in this study is considered to directly reflect the permeation properties of the membranes without the effect of the anode backing and catalyst layers. The q_M values of a side-chain type SPI membrane with an IEC of 1.94 mequiv. g^{-1} (abbreviated to SPI-SP hereafter) have been investigated at 80–100 °C and methanol concentrations of 3.2–9.6 wt.% by Watanabe and co-workers [21]. From their data, the q_M values for the SPI-SP at 60 °C were evaluated as 0.072×10^{-6} mol cm^{-2} s^{-1} and 0.15×10^{-6} mol cm^{-2} s^{-1} for 5 wt.% and 10 wt.% methanol, respectively, which were about a half of the q_M values for M4. The q_M values at 80 °C and 1.6 wt.% methanol for sulfonated poly(arylene ethers), BPSH-40 and 6FCN-35 with IECs of 1.72 mequiv. g^{-1} and 1.32 mequiv. g^{-1}, respectively, have been reported by Kim et al. [9]. Assuming the similar temperature dependence to the SPI membrane, the q_M values for BPSH-40 and 6FCN-35 at 60 °C and 5 wt.% methanol concentration were evaluated from their data as 0.24×10^{-6} mol cm^{-2} s^{-1} and 0.27×10^{-6} mol cm^{-2} s^{-1}, respectively, which were about two times larger than the q_M value for M4. Recently, Kim et al. also have reported the DMFC performance for sulfonated poly(arylene ether ether nitrile), m-SPAEEN-60, with an IEC of 1.91 mequiv. g^{-1} [9], of which the q_M value (0.064×10^{-6} mol cm^{-2} s^{-1} at 60 °C and 1.6 wt.% methanol concentration) was slightly larger than the corresponding value of M4.

The $p_{M,L/L}$ values were 4.4×10^{-6} cm^2 s^{-1} and 1.7×10^{-6} cm^2 s^{-1} for Nafion 112 and M2, respectively, at 60 °C and 10 wt.% methanol concentration, which were two times larger than the corresponding

Table 3
Methanol flux (q_M) of representative PEMs in DMFC operation.

Membrane	Thickness (μm)	Operation conditions			i (mA cm^{-2})	Ref.
		q_M (μmol cm^{-2} s^{-1})	Temp. (°C)	MeOH (wt.%)		
Nafion 117	180	0.19	50	4.8	0	5
		0.25	50	4.8	200	
		0.5	50	12.8	0	
		0.74	50	12.8	200	
Nafion 1135	90	0.10	50	1.6	0	
		0.07	50	1.6	200	
GEFC-117		0.32	60	6.5	0	6
		0.27	60	6.5	200	
Nafion 112	51	0.26	80	1.6	0	9
Nafion 115	127	0.14	80	1.6	0	
6FCN-35	51	0.13	80	1.6	0	
BPSH-40	49	0.15	80	1.6	0	
Nafion 112	50	0.19	60	1.6	0	13
m-SPAEEN-60	53	0.064	60	1.6	0	
		0.090	80	1.6	0	
		0.35	80	6.4	0	
Nafion 112	50	0.20	80	3.2	100	21
		0.53	80	6.4	100	
		0.87	80	9.6	100	
SPI-SP	50	0.077	80	3.2	100	
		0.16	80	6.4	100	
		0.25	80	9.6	100	
Nafion 112	55	0.53	60	5	200	This study
		1.22	60	10	200	
Nafion 115	130	0.82	60	10	200	
M4	53	0.12	60	5	200	
		0.29	60	10	200	

p_M values (2.1×10^{-6} cm^2 s^{-1} and 0.71×10^{-6} cm^2 s^{-1} for Nafion 112 and M2, respectively). The smaller values measured *in situ* compared with the values *ex situ* was due to the lower membrane swelling near the cathode in DMFC operation, where the membrane on the cathode was contact with humidified gas instead of water.

As mentioned above, the water and methanol crossover behavior is quite different between Nafion and SPI membranes. The methanol and water crossover increase significantly with increasing load current density for Nafion membranes, but not for SPI membranes. The methanol crossover is followed by the methanol electro-oxidation on cathode, which competes with the oxygen reduction on cathode, resulting in a mixed potential and a reduction of *OCV*. Therefore, under the conditions of a high methanol concentration and a high load current density, the total amount of water in the cathode became much larger for Nafion than for SPI membrane. This interrupts diffusion of oxygen molecules from gas diffusion layer to catalyst layer of cathode. As a result, oxygen diffusion into catalyst layer is apt to become a rate-determining step, especially for the air supply. This causes further reduction in DMFC performance, especially of maximum output, for Nafion membranes. In the case of SPI membranes, both the water and methanol fluxes are kept at a relatively low level even at a high current density and a high methanol concentration. As a result, the DMFC performance for SPI membranes is kept at a relatively high level.

3.4. Efficiency of DMFC

The Faraday's efficiency (η_F) is defined as the ratio of the methanol consumed for electrochemical reaction to the total methanol consumption including the methanol consumed for electrochemical reaction and wasted by crossover. The potential efficiency (η_E) is defined as the ratio of cell voltage to the standard cell voltage (E_o = 1.214 V). The overall DMFC efficiency (η_{DMFC}) is defined as the product of η_F and η_E. These are effective factors to evaluate the PEM performance in the DMFC operation. Table 2 summarizes the η_F, η_E and η_{DMFC} at a current density of 200 (or 400) mA cm^{-2} together with other DMFC performance factors such as *OCV*, $\sigma_{\perp,FC}$ and cell voltage $V_{200(400)}$.

Although the q_M and η_F hardly depended on the cathode gas, oxygen or air, the cell voltage, η_E and η_{DMFC} largely depended on it. They were larger for oxygen than for air. The differences in them between oxygen and air increased with increasing methanol feed concentration and current density and were larger for Nafion 112 than for SPI membranes. For 5 wt.% methanol and at 200 mA cm^{-2}, the η_{DMFC} values with air supply were 10.5% and 21% for Nafion 112 and M4, respectively, and the corresponding values with oxygen supply were 11.6% and 23%. The two times higher η_{DMFC} values for M4 were due to the 1.9 times higher η_F values. With an increase in methanol concentration, the η_F and η_{DMFC} decreased largely especially for Nafion membranes. For 20 wt.% methanol, Nafion membranes showed very low η_{DMFC} values of 3.3–4.1% even with the oxygen supply, whereas M4 showed fairly high η_{DMFC} values of 10.8% and 9.5% with oxygen and air supply, respectively. The three times higher η_{DMFC} values for M4 were due to the three times larger η_F values.

With increasing the current density from 200 mA cm^{-2} to 400 mA cm^{-2}, the η_F increased, but the η_E decreased, and as a result the η_{DMFC} increased or decreased depending on the operation conditions. In the case of a low methanol feed concentration of 5 wt.%, for SPI membrane, the increase in η_F at 400 mA cm^{-2} was not so

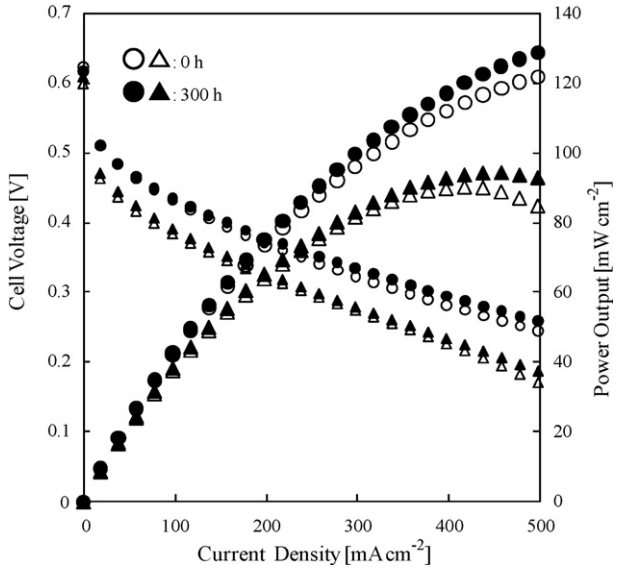

Fig. 9. DMFC performance for M3 (35 μm in thickness) before and after the durability test with supply of 10 wt.% methanol solution and dry gas at 60 °C. (○,●) O_2, 150 N cm^3 min^{-1}; (△, ▲) air, 450 N cm^3 min^{-1}.

large because of the fairly high η_F value of 75% at 200 mA cm^{-2} to compensate the decrease in η_E and as a result the η_{DMFC} at 400 mA cm^{-2} was smaller than that at 200 mA cm^{-2} regardless of the oxygen and air supply. In the case of a high methanol feed concentration (for example, 20 wt.%), for Nafion and SPI membranes, the increase in η_F was so large to compensate the small decrease in η_E with the oxygen supply and as a result the η_{DMFC} at 400 mA cm^{-2} was similar to that at 200 mA cm^{-2}. On the other hand, with the air supply, the decrease in η_E was larger and the η_{DMFC} at 400 mA cm^{-2} was smaller than that at 200 mA cm^{-2}.

Among the SPI membranes M1–M4, M4 showed the best η_{DMFC} performance. This is explained as follows. M4 had a low IEC of 1.51 mequiv. g^{-1} and a moderate thickness of 53 μm, which led to the low q_M and high η_F. M1 and M2 had high IECs of 1.96 mequiv. g^{-1} and 1.89 mequiv. g^{-1} and relatively thin thicknesses of 46 μm and 34 μm, which led to the relatively small cell resistance and large $\sigma_{\perp,FC}$ and also led to the relatively large q_M and low η_F. The former contributes to the lower *I–V* loss, but the latter acts to reduce the cell voltage. As a result, the V_{200} and the η_E were comparable between M1–2 and M4. Therefore, the lower q_M and higher η_F for M4 led to the higher η_{DMFC}.

3.5. Durability

A short-term durability test was performed for M3 of 35 μm in thickness at 60 °C for 300 h. Fig. 9 shows the polarization curves before and after the test. After the test for 300 h, the DMFC performance was rather improved, namely, the *OCV* and cell voltage and output power increased slightly after the test. This would be due to the improved catalyst activity. The MEA remained intact and there is no sign of property deterioration for the PEM, suggesting the good durability of this kind of SPI membranes for DMFC application at moderate temperatures.

4. Conclusions

The SPI membranes derived from NTDA and BAPBDS showed excellent tolerance against methanol and more than 2.5 times lower methanol permeability but 30–50% smaller through-plain proton conductivity in water than Nafion 112. The *OCV* was much higher for the SPIs than for Nafion 112 due to the lower methanol permeability. The methanol and water crossover through the SPI membranes during DMFC operation were controlled by only the molecular diffusion but not by the electro-osmotic drag. This was quite different from Nafion membranes and was of great advantage to DMFC performance. The SPI membranes displayed better DMFC performances than Nafion membranes especially at high methanol feed concentrations and with air supply. At a relatively low methanol feed concentration of 5 wt.% and 60 °C, the SPI membrane (M4, 53 μm) with a low IEC of 1.51 mequiv. g^{-1} showed the high DMFC performances, namely, V_{200} of 0.34 V and W_{max} of 88 mW cm^{-2}, which were comparable to those of Nafion 112. However, the η_{DMFC} value for M4 was 21% at 200 mA cm^{-2} due to a high η_F of 75%, which were two times higher than those of Nafion 112. At a high methanol feed concentration of 30 wt.%, Nafion 112 showed the too low cell performance to be measured stably, whereas M4 displayed moderately high cell performance, namely, *OCV* of 0.59 V, V_{200} of 0.25 V and W_{max} of 55 mW cm^{-2}. A short-term durability test for 300 h at 60 °C showed no deterioration in fuel cell performances for the SPI membrane. The SPI membranes have potential for DMFC applications at mediate temperatures.

Acknowledgements

This work was financially supported by the New Energy and Industrial Technology Development Organization (NEDO) and by a Grand-in-aid for Development Science Research (No. 19550209) from the Ministry of Education, Science and Culture of Japan.

References

[1] N.W. Deluca, Y.A. Elabd, J. Polym. Sci. Part B: Polym. Phys. 44 (2006) 2201–2225.
[2] V. Neburchilov, J. Martin, H.J. Wang, J.J. Zhang, J. Power Sources 169 (2007) 221–238.
[3] A. Heinzel, V.M. Barragan, J. Power Sources 84 (1999) 70–74.
[4] J. Ling, O. Savadogo, J. Electrochem. Soc. 151 (2004) A1604–A1610.
[5] S. Eccarius, B.L. Garcia, C. Hebling, J.W. Weidner, J. Power Sources 179 (2008) 723–733.
[6] A. Casalegno, R. Marchesi, J. Power Sources 185 (2008) 318–330.
[7] T. Schaffer, T. Tschinder, V. Hacker, J.O. Besenhard, J. Power Sources 153 (2006) 210–216.
[8] Y.A. Elabd, E. Napadensky, J.M. Sloan, J. Membr. Sci. 217 (2003) 227–242.
[9] Y.S. Kim, M.J. Sumner, W.L. Harrison, J.S. Riffle, J.E. McGrath, B.S. Pivovar, J. Electrochem. Soc. 151 (2004) A2150–2156.
[10] Y.Z. Fu, A. Manthiram, J. Power Sources 157 (2006) 222–225.
[11] M.L. Hill, Y.S. Kim, B.R. Einsla, J.E. McGrath, J. Membr. Sci. 283 (2006) 102–108.
[12] F. Lufrano, V. Baglio, P. Staiti, A.S. Arico, V. Antonucci, J. Power Sources 179 (2008) 34–41.
[13] Y.S. Kim, D.S. Kim, B. Liu, M.D. Guiver, B.S. Pivovar, J. Electrochem. Soc. 155 (2008) B21–B26.
[14] L. Li, J. Zhang, Y.X. Wang, J. Membr. Sci. 226 (2003) 159–167.
[15] V.S. Silva, B. Ruffmann, S. Vetter, M. Boaventura, A.M. Mendes, L.M. Madeira, S.P. Nunes, Electrochim. Acta 51 (2006) 3699–3706.
[16] Y. Yin, J.H. Fang, Y.F. Cui, K. Tanaka, H. Kita, K. Okamoto, Polymer 44 (2003) 4509–4518.
[17] K. Miyatake, H. Zhou, T. Matsuo, H. Uchida, M. Watanabe, Macromolecules 37 (2004) 4961–4966.
[18] B.R. Einsla, Y.S. Kim, M.A. Hickner, Y.T. Hong, M.L. Hill, B.S. Pivovar, J.E. McGrath, J. Membr. Sci. 255 (2005) 141–148.
[19] K. Okamoto, Y. Yin, O. Yamada, M.N. Islam, T. Honda, T. Mishima, Y. Suto, K. Tanaka, H. Kita, J. Membr. Sci. 258 (2005) 115–122.
[20] Y. Yin, O. Yamada, K. Tanaka, K. Okamoto, Polym. J. 38 (2006) 197–219.
[21] J.M. Song, K. Miyatake, H. Uchida, M. Watanabe, Electrochim. Acta 51 (2006) 4497–4504.
[22] F.X. Zhai, X.X. Guo, J.H. Fang, H.J. Xu, J. Membr. Sci. 296 (2007) 102–109.
[23] C. Xu, T.S. Zhao, J. Power Sources 168 (2007) 143–153.
[24] T. Watari, J.H. Fang, X.X. Guo, K. Tanaka, H. Kita, K. Okamoto, T. Hirano, J. Membr. Sci. 230 (2004) 111–120.
[25] X.X. Guo, J.H. Fang, T. Watari, K. Tanaka, H. Kita, K. Okamoto, Macromolecules 35 (2002) 6707–6713.
[26] Y. Yin, Y. Suto, T. Sakabe, S.W. Chen, S. Hayashi, T. Mishima, O. Yamada, K. Tanaka, H. Kita, K. Okamoto, Macromolecules 39 (2006) 1189–1198.
[27] Z. Hu, Y. Yin, K. Yaguchi, N. Endo, M. Higa, K. Okamoto, Polymer 50 (2009) 2933.
[28] T. Tschinder, T. Schaffer, S.D. Fraser, V. Hacker, J. Appl. Electrochem. 37 (2007) 711–716.
[29] H. Dohle, J. Divisek, J. Mergel, H.F. Oetjen, C. Zingler, D. Stolten, J. Power Sources 105 (2002) 274–282.